Protective effects of flavonoids from the leaves of *Carya cathayensis* Sarg. against H_2O_2-induced oxidative damage and apoptosis *in vitro*

FANG-MEI ZHOU[1*], JING-JING HUANG[1*], XU-JIAO HU[2], JINGWEI WANG[3], BING-QI ZHU[1], ZHI-SHAN DING[1], SHIGAO HUANG[4] and JING-JING FANG[2]

[1]Technology Teaching Center of Medical Laboratory and Quarantine, School of Medical Technology and Information Engineering, Zhejiang Chinese Medical University, Hangzhou, Zhejiang 310053; [2]Inspection Department, Yinzhou People's Hospital, Ningbo, Zhejiang 315040; [3]Department of Pathology, Academy of Chinese Medical Sciences, Zhejiang Chinese Medical University, Hangzhou, Zhejiang 310053; [4]Faculty of Health Sciences, University of Macau, Taipa 999078, Macau SAR, P.R. China

Received February 7, 2021; Accepted September 27, 2021

DOI: 10.3892/etm.2021.10878

Abstract. Hydrogen peroxide (H_2O_2) can induce apoptosis by releasing reactive oxygen species (ROS) and reactive nitrogen species, which cause mitochondrial damage. The present study aimed to investigate the protective effects of flavonoids from the leaves of *Carya cathayensis* Sarg. against H_2O_2-induced oxidative damage and apoptosis *in vitro*. The bioactivity of total flavonoids (TFs) and five monomeric flavonoids [cardamonin (Car), pinostrobin chalcone, wogonin, chrysin and pinocembrin] from the leaves of *Carya cathayensis* Sarg. (LCCS) were tested to prevent oxidative damage to rat aortic endothelial cells (RAECs) induced by H_2O_2. Oxidated superoxide dismutase, glutathione peroxidase, malondialdehyde, lactate dehydrogenase and ROS were analyzed to evaluate the antioxidant activity. Gene and protein expression patterns were assessed using reverse transcription-quantitative PCR and western blotting, respectively. The results indicated that TFs and Car inhibited H_2O_2-induced cytotoxicity and apoptosis of RAECs. Additionally, they regulated the level of oxidase and inhibited the production of ROS. Overall, the TFs extracted from LCCS could potentially be developed as effective candidate drugs to prevent oxidative stress in the future; moreover, they could also provide a direction in investigations for preventing antioxidant activity through the ROS pathway.

Correspondence to: Dr Shigao Huang, Faculty of Health Sciences, University of Macau, 22-3022 Avenida da Universidade, Taipa 999078, Macau SAR, P.R. China
E-mail: huangshigao2010@aliyun.com

Dr Jing-Jing Fang, Inspection Department, Yinzhou People's Hospital, 251 Baizhang East Road, Ningbo, Zhejiang 315040, P.R. China
E-mail: jjf0311@163.com

*Contributed equally

Key words: total flavonoid, reactive oxygen species, *Carya cathayensis* Sarg., apoptosis, oxidative stress, Akt/MAPKs

Introduction

Vascular pathologies rank amongst the most life-threatening diseases in the world, and the cause of the majority of these vascular pathologies is dysfunctional endothelial cells (1). Endothelial cells cover the inner surface of all blood vessels and play a notable role in maintaining normal vascular function, regulating blood circulation and exchanging substances in blood (2). Oxidative stress refers to the cytopathological consequences when cells are exposed to a high concentration of oxygen or chemical derivatives of oxygen (3), which are among the factors that induce endothelial dysfunction (4). Oxidative stress is associated with the occurrence and development of cardiovascular diseases such as hypertension, atherosclerosis and heart failure (5). Therefore, protecting endothelial cells from oxidative injury and apoptosis represents a beneficial strategy for the treatment of vascular diseases. At present, the majority of antioxidant drugs are chemical drugs. These chemicals have some limitations, including varying degrees of toxicity, residual effects, deformities and potential carcinogenicity. Therefore, it is of great clinical significance to screen effective and safe natural oxygen free radical scavengers as substitutes for synthetic antioxidants.

Natural products have been a rich source of compounds for drug discovery and represent attractive alternatives for disease prevention and treatment (6,7). To date, numerous studies have been conducted to find effective drugs to block oxidative damage (4,8). The ability of various bioactive flavonoids from natural products and traditional Chinese medicine to scavenge free radicals have been reported (9,10). Wen *et al* (11) have demonstrated that flavonoids extracted from Traditional Chinese medicine and natural plants are broad-spectrum free radical scavengers that can effectively eliminate free radicals in the body and play an antioxidant role (11). Chen *et al* (12) identified 12 flavonoid components in

lotus plumule and demonstrated their significant antioxidant activity. Wei *et al* (13) isolated ten flavonoid derivatives from the fruits of *Metaplexis japonica*, whose antibacterial and antioxidant activities were also revealed in their study.

Carya cathayensis Sarg., a deciduous tree belonging to the hickory family, has been widely used as a conventional folk medicine for thousands of years. It was commercially cultivated in the Zhejiang and Anhui provinces of China (14). The effectiveness of the anticancer, free radical scavenging, cardiotonic, anti-inflammatory and antinociceptive actions of the husk and kernel of *Carya cathayensis* Sarg. was reported (15); however, the value of the leaves of *Carya cathayensis* Sarg. (LCCS) remains sparsely investigated. In our previous study, total flavonoids (TFs) were demonstrated to be abundant in the LCCS (16), and five flavonoid monomers, cardamonin (Car), pinostrobin chalcone (PC), wogonin (Wo), chrysin (Chr) and pinocembrin (Pin) (Fig. 1) were separated from the TFs (17). In addition, the pharmaceutical properties of TFs, for example, anti-inflammatory activity (12), anti-tumor activity (18), anti-early atherosclerosis lesion formation *in vivo* (19) and anti-human umbilical vein endothelial cell senescence (13) have been investigated. However, the activities of flavonoids from LCCS against H_2O_2-induced oxidative damage *in vitro* remain poorly investigated.

The present study aimed to investigate the potential antioxidant effects of TFs and flavonoid monomers from LCCS on H_2O_2-induced oxidative damage in rat aortic endothelial cells (RAECs). Fig. 2 describes the mechanisms by which the TFs and Car from LCCS protect against H_2O_2-induced apoptosis.

Materials and methods

Materials and regents. LCCS was obtained in 2016 from Lin'an (Zhejiang, China). The plants were authenticated by Professor Zhishan Ding from Zhejiang Chinese Medical University, Hangzhou, Zhejiang,China. The voucher specimens were deposited in the laboratory center of the Medical Technology College at Zhejiang Chinese Medical University (Hangzhou, China; voucher no. LCC-20160915-G). The TFs were extracted from LCCS according to the method described in our previous study (17). Analytical grade H_2O_2 was purchased from Sinopharm Chemical Reagent Co., Ltd. PC and Pin were further separated and purified from TFs. Car, Wo and Chr were obtained from Shanghai Yuanye Biotechnology, Co., Ltd. and Beijing Aoke Biological Technology Co., Ltd. Malondialdehyde (MDA; cat. no. A003-4-1), superoxide dismutase (SOD; cat. no. A001-3-2), lactate dehydrogenase (LDH; cat. no. A020-2-2) and glutathione peroxidase (GSH-Px; cat. no. A005-1-2) assay kits were all purchased from Nanjing Jiancheng Bioengineering Institute. A FITC Annexin V apoptosis detection kit was purchased from BD Biosciences (cat. no. 556547). Antibodies against caspase-3 (cat. no. YM3431), Bax (cat. no. YT0455), Bcl-2 (cat. no. YT0470), β-actin (cat. no. YM3028), Akt (cat. no. YT6111), phosphorylated (p)-Akt (cat. no. YP0590), ERK (cat. no. YT1624), p-ERK (cat. no. YP0101), JNK (cat. no. YT2441), p-JNK (Thr183/Tyr185; cat. no. YP0157), p38 (cat. no. YT3514) and p-p38 MAPK (Thr180/Tyr182; cat. no. YP0338) were supplied by ImmunoWay Biotechnology Company. Horseradish peroxidase-conjugated goat anti-rabbit IgG (cat. no. abs20002) and goat anti-mouse IgG (cat. no. abs20003) were purchased from Aibixin (Shanghai) Biotechnology Co., Ltd. An MTS assay kit (cat. no. G3580) with 3-(4,5-dimethylthiazoll-2-yl)-5-(3-carboxymethoxyphenyl)-2-(4-sulfophenyl)-2H-tetrazolium reagent and an inner salt was purchased from Promega Corporation. A First Strand complementary (c)DNA Synthesis kit was used (Takara Bio, Inc.) and SYBR® Premix Ex Taq™ II were purchased from Takara Bio, Inc.

Cell culture. The RAECs were purchased from Yingwan Biotechnology Co., Ltd. (cat. no. C3048) The RAECs were cultured in DMEM supplemented with 10% heat-inactivated FBS (cat. no. 70220-8611; Zhejiang Tianhang Biotechnology Co., Ltd.), 100 mg/ml streptomycin and 100 U/ml penicillin at 37˚C in a humidified 5% CO_2 incubator.

Determination of TFs and the concentrations of five flavonoids using MTS assay. The effects of TFs and five flavonoids (Car, PC, Won, Chr and Pin) on the proliferation of RAEC cell lines were evaluated using the MTS assay. Briefly, cells were seeded in 96-well plates at a density of $1.5x10^5$ cells/well in phenol-free red DMEM/F12 (1:1) medium with 10% CS-FBS purchased from Biosharp Biotechnology Co., Ltd (cat. no. BL305A). After incubation at 37˚C for 24 h, the cells were treated with TFs at 0, 5, 10, 20, 40 and 80 μg/ml, or the five flavonoids (Car, PC, Won, Chr and Pin) at 0, 5, 10, 20, 40 and 80 μM for 24 h. Subsequently, 20 μl of MTS solution was added to each well and incubated for an additional 2 h at 37˚C in a CO_2 incubator. The absorbance values were detected by a microplate reader (Dynatech Nevada, Inc.) at 490 nm. The average cell activity was calculated according to the following formula: Percentage of cell viability = [optical density (OD) of TFs and five flavonoid cells/OD of control cells] x100. The oxidative stress injury model induced by H_2O_2 was established using the MTS assay. Briefly, RAECs were cultured in a 96-well microtiter plate at a density of $1.5x10^5$ cells/well at 37˚C for 24 h. After that, RAECs were exposed to H_2O_2 (0, 50, 100, 150, 200 or 400 μM) for 24 h. Subsequently, RAECs were treated with appropriate H_2O_2 concentrations for 0, 2, 4, 6 and 8 h. Cell viability was measured by MTS assay as aforementioned.

Cell viability assay. RAECs were cultured in a 96-well microtiter plate at a density of $1.5x10^5$ cells/well for 24 h, and the cells were divided into the following five groups: i) Control group; ii) model group; iii) quercetin (Que) group (20 μM); iv) TF group (5 μg/ml, 10 μg/ml, 20 μg/ml); v) five flavonoids group (5, 10 and 20 μM). Subsequently, the RAECs were treated with TFs and five flavonoids at 37˚C for 24 h, followed by 100 μM H_2O_2 treatment at 37˚C for 2 h to establish an injury model. Control group cells were cultured with 200 μl of complete medium. Quercetin was used as a positive control (20). Briefly, 20 μl of MTS solution was added to each well and incubated for an additional 2 h at 37˚C in a CO_2 incubator. The absorbance values were detected by a microplate reader (Dynatech Nevada, Inc.) at 490 nm. The morphology of the cells was observed using a Nikon ECLIPSE Ti fluorescence inverted microscope (magnification, x20; Nikon Instruments Inc.), and images were captured.

Determination of intracellular MDA, LDH, SOD, and GSH-Px. To assess the effects of TFs and Car on oxidative injury in

Table I. List of primer sequences used in the present study.

Primer name	Sequence, (5'-3')	Length, bp	Ta, ˚C
Rat GAPDH forward	CCC ACG GCA AGT TCA ACG GCA	21	63.9
Rat GAPDH reverse	TGG CAG GTT TCT CCA GGC GGC	21	65.8
Rat Caspase-3 forward	CTG GAC TGC GGT ATT GAG	18	57.3
Rat Caspase-3 reverse	GGG TGC GGT AGA GTA AGC	18	59.6
Rat Bax forward	GCA AAC TGG TGC TCA AGG	18	57.3
Rat Bax reverse	TCC CGA AGT AGG AAA GGA G	19	57.6
Rat Bcl-2 forward	TCT AAC ATC CCA GCT TCA T	19	53.2
Rat Bcl-2 reverse	GCA ATC CGA CTC ACC AAT A	19	55.4

Ta, annealing temperature.

RAECs, RAECs were plated in a six-well plate at a density of $1.5x10^5$ cells/ml (2.5 ml/well) and cultured as described above. After pretreatment with TFs or Car for 24 h, cells were exposed to H_2O_2 for 2 h at 37˚C. The supernatant of each group was collected to evaluate the LDH and MDA levels. The cells in each group were digested and collected with 0.25% trypsin, and the cell homogenate was obtained by ultrasonic crushing. The adherent cells were lysed and then centrifuged at 4˚C and 12,000 x g for 15 min to collect the supernatant. The activities of SOD and GSH-Px were measured according to the manufacturer's instructions for the assay kits.

Apoptosis analysis by flow cytometry. An Annexin V-FITC detection kit was used to determine the effects of TFs and Car on apoptosis induced by H_2O_2. Briefly, cells were seeded into a six-well plate and treated as described above. After harvesting by trypsin, the cells were washed twice with precooled PBS, centrifuged at 4˚C and 500 x g/min for 5 min to remove the cell debris, and then re-suspended in 1X binding buffer. A 100 μl cell suspension was placed in a 5 ml flow tube, and the cells were stained with FITC Annexin V and propidium iodide (PI) for 15 min at room temperature. Cells were quantified using flow cytometry (BD Biosciences; Accuri C6) within 1 h. The percentage distributions of normal (viable), early apoptotic, late apoptotic and necrotic cells were calculated using Summit software (FCS Express 5; version 3.0).

Reverse transcription-quantitative PCR (RT-qPCR). RAECs were treated with 5, 10 and 20 μg/ml of TFs, and 5, 10 and 20 μM of Car for 24 h, followed by 100 μM H_2O_2 treatment for 2 h to establish an injury model. Total cell RNA was extracted using TRIzol® (Invitrogen; Thermo Fisher Scientific, Inc.) according to the manufacturer's instructions. The instructions of the First Strand cDNA Synthesis kit were followed to synthesize cDNA by RT-PCR. SYBR Green real-time fluorescent quantitative PCR was used to detect the mRNA expression levels of caspase-3, Bax and Bcl-2 in each group of cells, and the reactions were carried out using Step One Plus Real-Time PCR (Applied Biosystems; Thermo Fisher Scientific, Inc.). The reaction system was SYBR Premix EX Taq™ II 10 μl, upstream primer 0.5 μl, downstream primer 0.5 μl, cDNA 0.5 μl and ddH_2O 8.5 μl. The reaction condition were 95˚C for 5 min and then 40 cycles of 95˚C for 20 sec, 55˚C for 20 sec and 72˚C for 15 sec. The primers used are listed in Table I and were synthesized by Shanghai Shenggong Biology Engineering Technology Service, Ltd. All experimental procedures were in accordance with the manufacturer's protocols. The expression of mRNA was analyzed by the $2^{-\Delta\Delta Cq}$ method (21).

Western blotting. Total cytosolic protein of RAECs cultured with various concentrations of TFs and Car for 24 h and injured by H_2O_2 for 2 h as aforementioned. Cells were washed twice with cold PBS and lysed by cold lysis buffer (RIPA:PMSF=100:1) for 40 min on ice. Cell lysates were centrifuged at 12,000 x g for 15 min at 4˚C. The protein concentration was determined using a BCA protein assay kit according to the manufacturer's instructions. Harvested proteins were denatured at 100˚C for 10 min, 50 μg of protein/per lane from each sample was electrophoresed by SDS-PAGE and then transferred onto PVDF membranes. Membranes were blocked with 5% non-fat milk in TBS with 0.5% Tween-20 at room temperature for 2 h, followed by overnight incubation at 4˚C with primary antibodies (caspase-3, Bax, Bcl-2, β-actin, Akt, ERK, JNK, p38 MAPK, p-ERK, p-JNK and p-p38 MAPK) at a dilution of 1:1,000. Subsequently, the blots were incubated with horseradish peroxidase-conjugated goat anti-rabbit IgG (1:5,000) for 2 h at room temperature and detected using an enhanced chemiluminescence system. The bands were quantified by densitometry analysis with ImageJ software (National Institutes of Health; version, 1.8.0.112).

Statistical analysis. All studies were performed with three independent experiments. All data were analyzed using GraphPad Prism 8.0 software (GraphPad Software, Inc.). The data are expressed as the means ± standard deviation for continuous variables. Comparisons between groups were performed using one-way ANOVA, and normally distributed data were analyzed using Tukey's multiple comparisons post hoc test. Non-normally distributed data were analyzed using Dunn's test for intergroup comparisons. $P<0.05$ was considered to indicate a statistically significant difference.

Results

TFs and five monomeric flavonoids inhibit H_2O_2-induced injury in RAECs. As presented in Fig. 3A, treatment with 0-400 μM

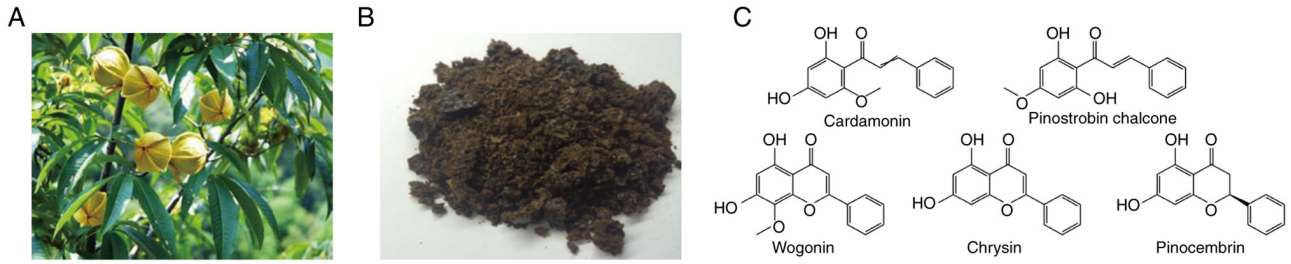

Figure 1. *Carya cathayensis* Sarg. and flavonoids. (A) *Carya cathayensis* Sarg. (B) Total flavonoids isolated from the leaves of *Carya cathayensis* Sarg. (C) Chemical structures of the five monomeric flavonoids.

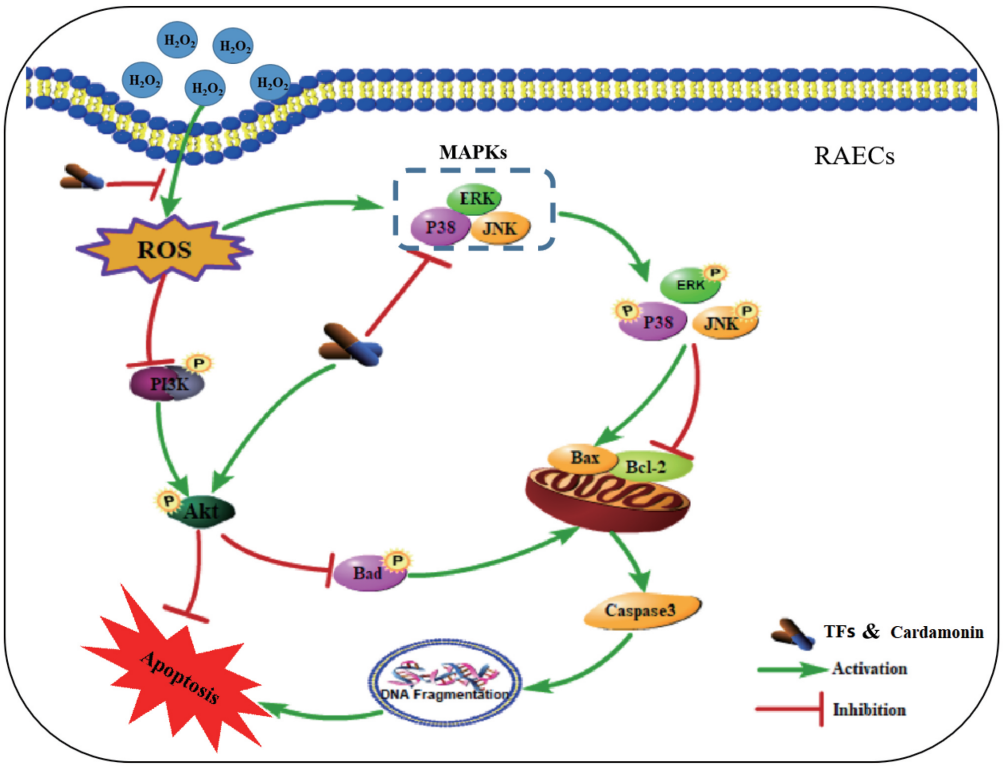

Figure 2. Proposed mechanisms by which TFs and Car from LCCS protect against H_2O_2-induced apoptosis. TFs and Car protect against H_2O_2-induced oxidative damage in RAECs by decreasing ROS generation, maintaining the intracellular redox balance, activating the Akt pathway and inhibiting the MAPK apoptotic pathways. TFs, total flavonoids; LCCS, leaves of *Carya cathayensis* Sarg.; Car, cardamonin; ROS, reactive oxygen species; p, phosphorylation; RAECs, rat aortic endothelial cells.

H_2O_2 for 24 h significantly decreased the survival rate of RAECs in a concentration-dependent manner (P<0.01). The cell viability decreased to 54.73±4.91% when the concentration of H_2O_2 increased to 100 μM. As presented in Fig. 3B, the cell viability decreased to 61.83±2.73% after 2 h of treatment, which was significantly different compared with that of the untreated group (P<0.01). Based on these results, 100 μM H_2O_2 for 2 h was selected as the treatment condition for the following experiments.

The results demonstrate that treatments with TFs and five monomeric flavonoids (Car, PC, Wo, Chr and Pin) at concentrations >40 μg/ml and 40 μM, respectively, inhibited cell proliferation compared with the control groups (P<0.01). Therefore, the optimal treatment concentrations for TFs (5, 10 and 20 μg/ml) and five monomeric flavonoids (5, 10 and 20 μM) were selected for subsequent experiments (Fig. 3C).

To assess the protective effects of TFs and five monomeric flavonoids on H_2O_2-induced injury, RAECs were pretreated with TFs (5, 10 or 20 μg/ml) and five monomeric flavonoids (5, 10 or 20 μM) for 24 h before exposure to 100 μM H_2O_2 for 2 h. As presented in Fig. 3D, the rate of cell viability was significantly decreased in the model group compared with the control group (P<0.01), and the cell viability after pretreatment with TFs and Car was significantly higher compared with that of the model group. TFs and Car displayed a protective effect that was close to that of quercetin (the positive control). However, a protective effect was not observed in cells treated with Wo, PC, Chr and Pin. Therefore, TFs and Car were selected for further antioxidant and antiapoptotic studies.

The morphologies of the cells were spindle shaped with clear and bright boundaries in the control group. In the H_2O_2 group, large numbers of suspended cells and cell fragments were observed. In the cells pretreated with TFs and Car, the shrinkage of cells decreased and few suspended cells and cell fragments were observed. The protective effect was

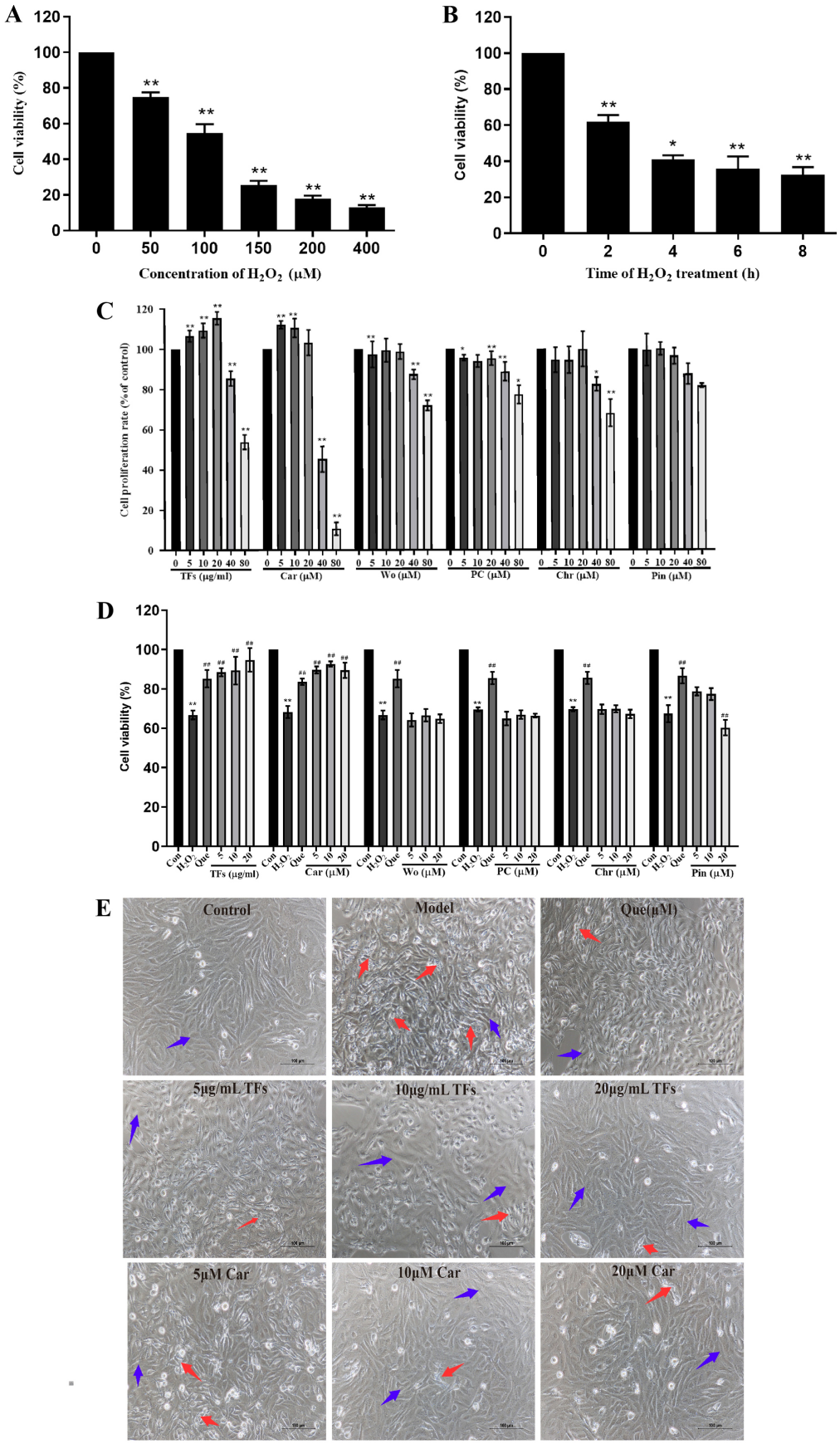

Figure 3. TFs and five monomeric flavonoids inhibit H_2O_2-induced injury in RAECs. (A) RAECs were treated with increasing concentrations of H_2O_2 (0-400 μM) for 2 h and cell viability was assessed. (B) RAECs were treated with 100 μM H_2O_2 for 0-8 h. (C) Effects of increasing concentrations of TFs and five monomeric flavonoids on the proliferation rate of RAECs. (D) Protective effects of increasing concentrations of TFs and five monomeric flavonoids on H_2O_2-induced RAEC damage. (E) Effects of TFs and Car on the morphology of RAECs after H_2O_2-induced injury (magnification, x200; scale bar, 100 μm) n=6. *P<0.05, **P<0.01 vs. control group. $^{\#\#}$P<0.01 vs. H_2O_2 model group. RAECs, rat aortic endothelial cells; TFs, total flavonoids; Car, cardamonin; Wo, wogonin; PC, pinostrobin chalcone; Chr, chrysin; Pin, pinocembrin; Que, quercetin; Con, control.

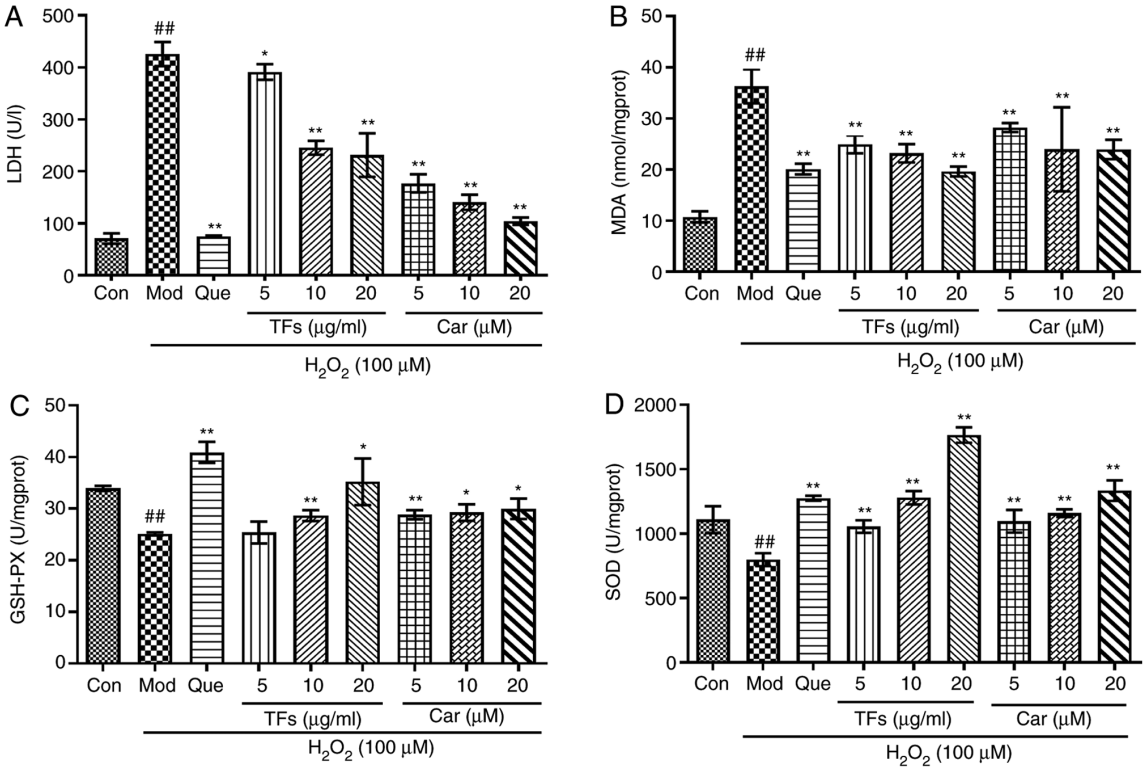

Figure 4. Protective effects of TFs and flavonoids by modulating the activities of enzymes. (A) Level of LDH released in RAECs. (B) Content of intracellular MDA. (C) Activities of GSH-PX and (D) SOD. n=3. $^{\#\#}$P<0.01 vs. control group; *P<0.05, **P<0.01 vs. H_2O_2 model group. TFs, total flavonoids; LDH, lactate dehydrogenase; RAECs, rat aortic endothelial cells; MDA, malondialdehyde; GSH-PX, glutathione peroxidase; SOD, super oxide dismutase; Con, control; Mod, model; Que, quercetin; Car, cardamonin.

dose-dependent, and its effect was similar to that of quercetin (Fig. 3E).

Effect of TFs and Car on LDH, MDA, GSH-Px and SOD levels. To determine the effects of TFs and Car on oxidative stress in RAECs, the levels of LDH, MDA, GSH-Px and SOD were measured. As presented in Fig. 4A and B, the levels of LDH and MDA in the supernatant of the model group were significantly increased compared with those in the control group (P<0.01). Compared with the model group, treatment with TFs and Car significantly reduced the production of LDH and MDA in a dose-dependent manner (P<0.05). In the model group, the contents of GSH-Px and SOD were significantly reduced compared with those in the control group (P<0.01). After pretreatment with TFs and Car, the activity of GSH-Px and SOD was markedly increased compared with that of the model group (Fig. 4C and D).

TFs and Car suppresses H_2O_2-induced intracellular ROS production. Intracellular ROS play an important role in oxidative stress-induced cell damage. In the model group, intracellular ROS generation was significantly increased by >3.8-fold compared with that in the control group (P<0.01; Fig. 5). In contrast, the relative fluorescence intensities were reduced by 1.04±0.05, 1.36±0.05 and 1.60±0.06 in the 5, 10 and 20 μg/ml TF-pretreated groups, and by 1.26±0.04, 1.34±0.02 and 1.55±0.06 in the 5, 10 and 20 μM CAR-pretreated groups, respectively. Therefore, pretreatment with TFs and Car prevented the elevation of ROS levels in a dose-dependent manner (P<0.01; Fig. 5).

Effect of TFs and Car on apoptosis in H_2O_2-induced RAECs. As presented in Fig. 6A, the apoptosis scatter plot can be divided into four quadrants: Upper left quadrant R1 (Annexin V-FITC)$^-$/PI$^+$, which refers to mechanically injured cells or a few late apoptotic cells; upper right quadrant R2 (Annexin V-FITC)$^+$/PI$^+$, for late apoptotic cells; lower left quadrant R3 (Annexin V-FITC)$^-$/PI$^-$, normal living cells; and the lower right quadrant R4 (Annexin V-FITC)$^+$/PI$^-$, which presents early apoptotic cells. The total apoptotic cells were the sum of early apoptotic cells and late apoptotic cells. As presented in Fig. 6B, in the normal control group, only a few cells were apoptotic and the apoptosis rate was 9.31±1.84%. Compared with the normal control group, large numbers of apoptotic cells and fragments were revealed in the H_2O_2 model group, and the apoptosis rate was 28.71±4.41% (P<0.01). Compared with the model group, the apoptotic rate of cells pretreated with TFs and Car resulted in a significant decrease (P<0.01). These results indicated that TFs and Car could inhibit the cell damage and apoptosis induced by H_2O_2.

TFs and Car downregulates apoptosis-related gene and protein expression levels in RAECs. To elucidate the molecular mechanism of the protective effect of TFs and Car against H_2O_2-induced oxidative damage in RAECs, the mRNA expression of apoptosis-related genes, including caspase-3, Bax and Bcl-2, were investigated. Compared with the control group, the relative expression levels of caspase-3 and Bax mRNA in the model group were significantly increased (P<0.01; Fig. 7A and B). Pretreatment with TFs and Car for 24 h significantly inhibited the mRNA expression

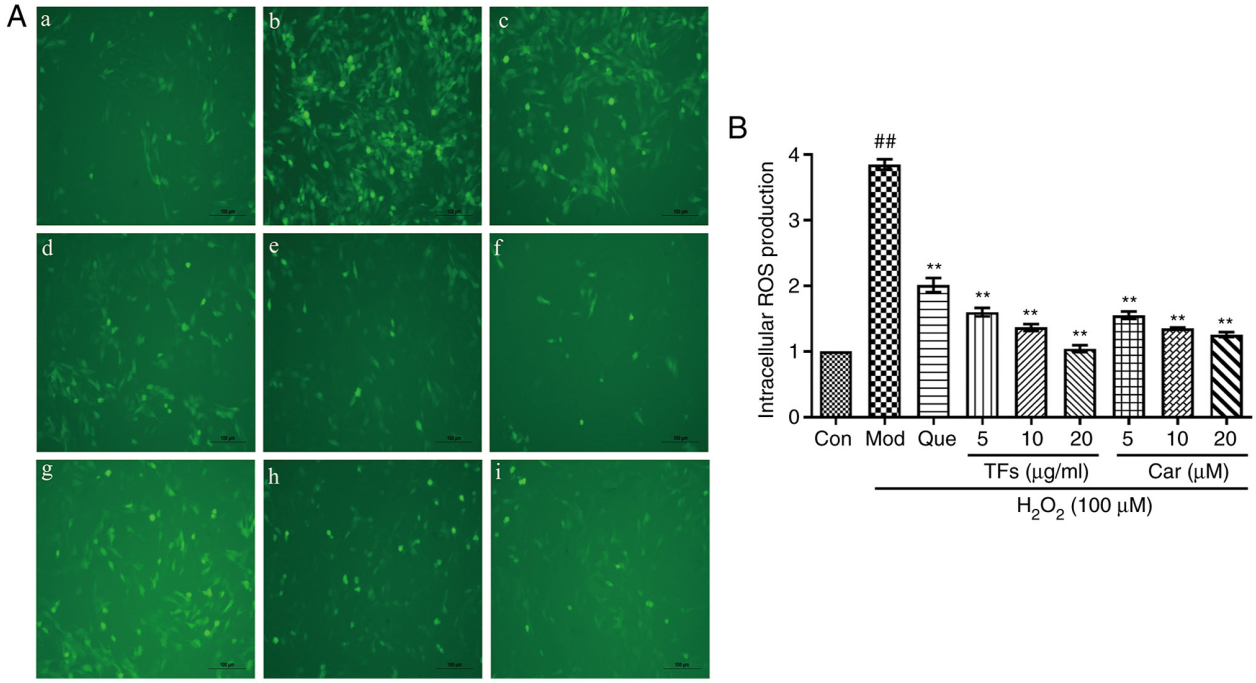

Figure 5. Protective effects of TFs and Car by reducing intracellular ROS induced by H_2O_2. (A) ROS generation was measured. Representative images of RAECs loaded with DCFH-DA (10 μM) were captured using a fluorescence microscope (magnification, x200). (a) Control group, (b) Model group, (c) quercetin group, (d) 5 μg/ml TFs group, (e) 10 μg/ml TFs group, (f) 20 μg/ml TFs group, (g) 5 μM Car group, (h) 10 μM Car group and (i) 20 μM Car group. (B) Quantitative analysis of DCF fluorescence intensity. n=3. $^{\#\#}$P<0.01 vs. control group; **P<0.01 vs. H_2O_2 model group. TFs, total flavonoids; RAECs, rat aortic endothelial cells; Con, control; Mod, model; Que, quercetin; Car, cardamonin.

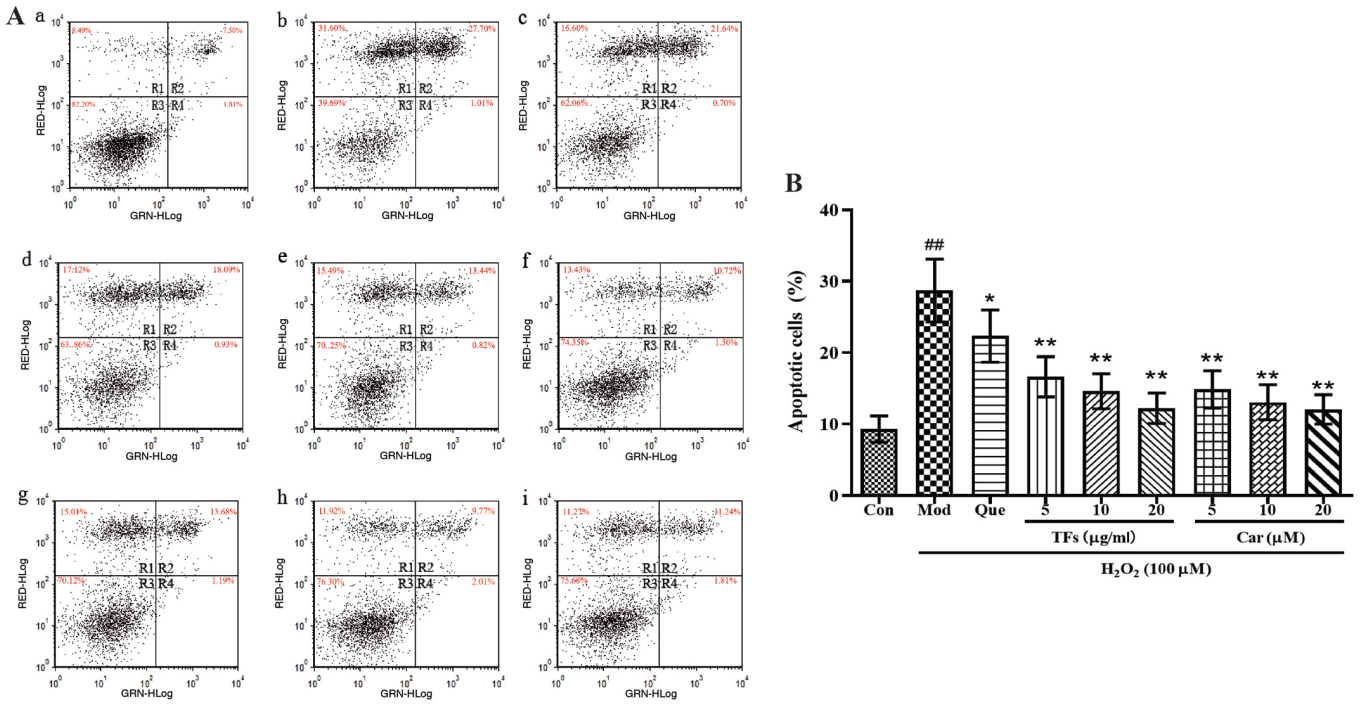

Figure 6. Effects of TFs and Car on H_2O_2-induced RAEC apoptosis. (A) Apoptosis was examined using Annexin V/PI staining followed by flow cytometry. R1, PI-positive cells (necrotic); R2, Annexin V-FITC-positive and PI-positive cells (late apoptotic/necrotic); R3, Annexin V-FITC-negative and PI-negative cells (normal viable cells); R4, Annexin V-FITC-positive and PI-negative cells (early apoptosis); total apoptotic cells are the sum of early apoptotic cells and late apoptotic cells. (a) Control group, (b) Model group, (c) quercetin group, (d) 5 μg/ml TFs group, (e) 10 μg/ml TFs group, (f) 20 μg/ml TFs group, (g) 5 μM Car group, (h) 10 μM Car group, (i) 20 μM Car group. (B) Percentages of apoptotic cells were calculated. n=3. $^{\#\#}$P<0.01 vs. control group; *P<0.05, **P<0.01 vs. H_2O_2 model group. TFs, total flavonoids; Car, cardamonin; RAECs, rat aortic endothelial cells; PI, propidium iodide; Con, control; Mod, model; Que, quercetin.

levels of caspase-3 and Bax compared with the model group in a dose-dependent manner (P<0.01); furthermore, its effect was similar to that of the positive control drug, quercetin. In addition, the relative expression of Bcl-2 mRNA in the model

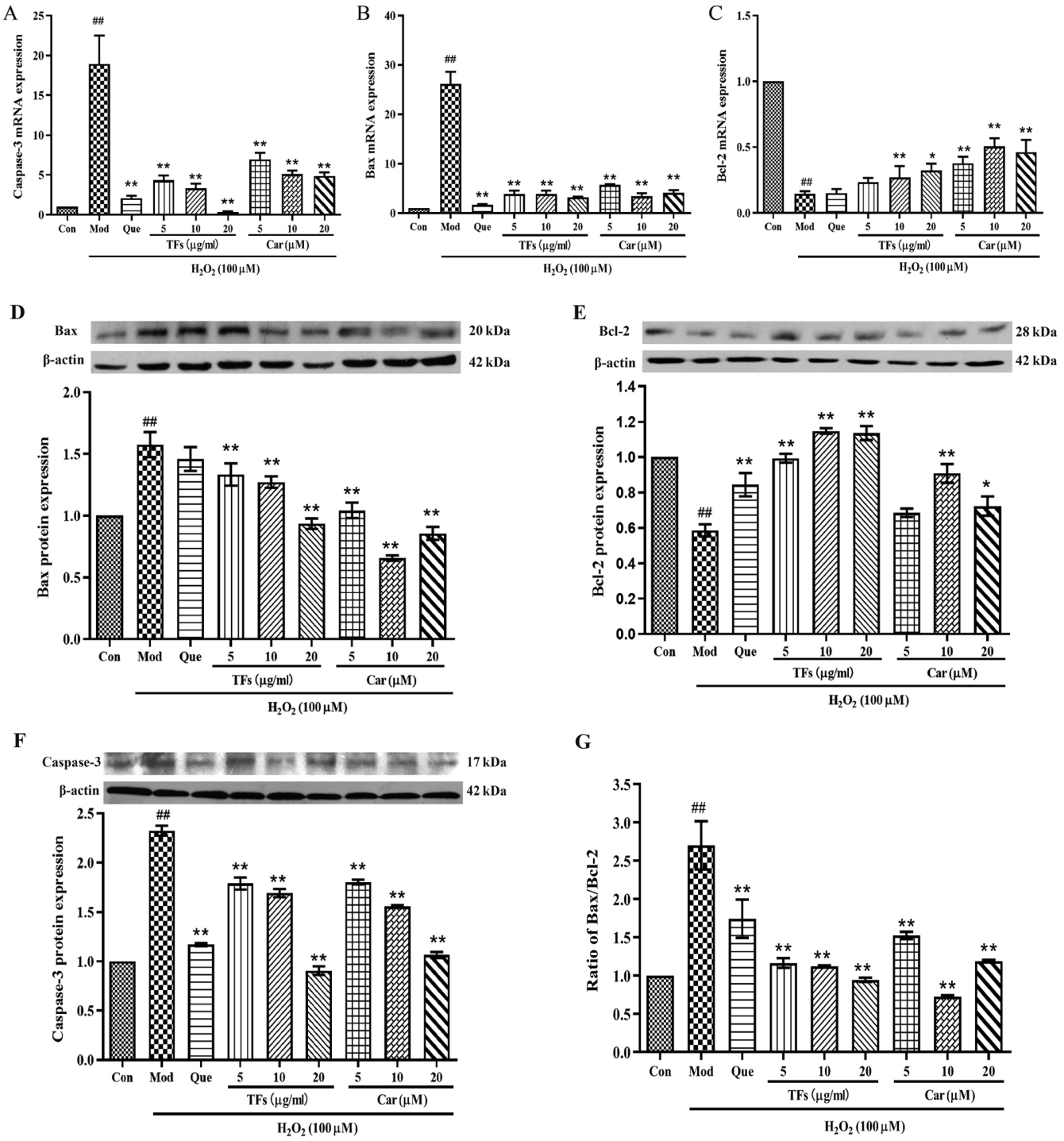

Figure 7. Effects of TFs and Car on the expression of apoptosis-related genes and proteins in oxidative damage of RAECs. (A) Effects on the expression of caspase-3 mRNA. (B) Effects on the expression of Bax mRNA. (C) Effects on the expression of Bcl-2 mRNA. Expression levels of (D) Bax, (E) Bcl-2 and (F) caspase-3 protein in RAECs treated with TFs and Car were estimated using western blotting. (G) Ratio between Bcl-2 and Bax proteins. β-actin was used as the protein loading control. n=3. $^{\#\#}$P<0.01 vs. control group; *P<0.05, **P<0.01 vs. H_2O_2 model group. TFs, total flavonoids; Car, cardamonin; RAECs, rat aortic endothelial cells; Con, control; Mod, model; Que, quercetin.

group was significantly lower compared with that in the control group (P<0.01; Fig. 7C). Compared with the model group, cells pretreated with TFs and Car for 24 h significantly reduced the H_2O_2-induced inhibition of Bcl-2 mRNA expression (P<0.01), and both TFs and Car exhibited superior effects relative to quercetin (Fig. 7C).

Next, the expression of apoptosis-related proteins were examined, including caspase-3, Bcl-2 and Bax, using western blotting. Compared with the control group, H_2O_2 treatment caused significantly increased protein expression levels of caspase-3 (Fig. 7F) and Bax (Fig. 7D), and decreased protein expression of Bcl-2 (Fig. 7E) in the model group. By contrast, treatment with TFs significantly inhibited the elevation of caspase-3 and Bax protein levels while upregulating the expression of Bcl-2 protein compared with the control group (P<0.01). Similar effects were observed when cells were

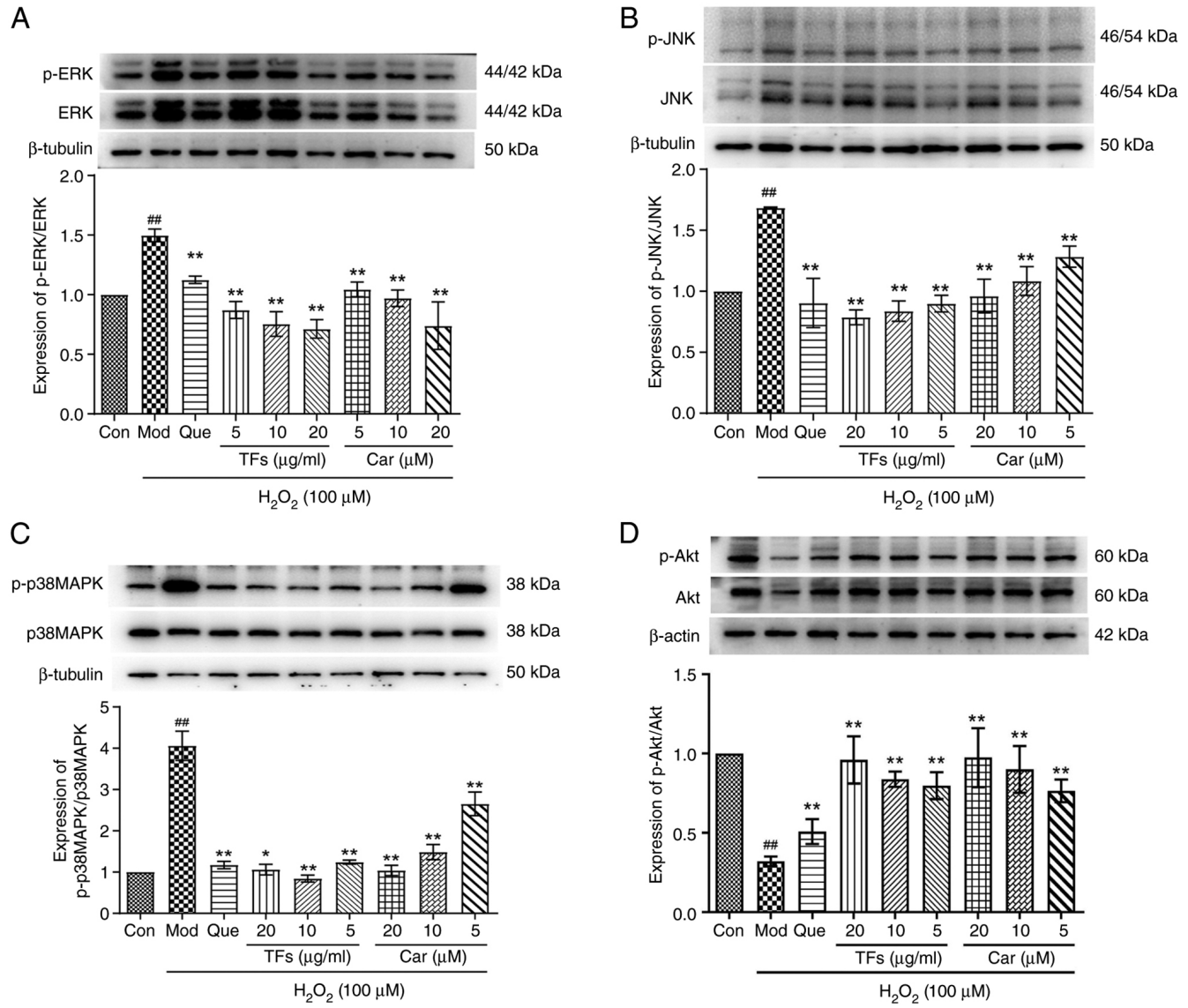

Figure 8. Effects of TFs and Car on the AKT and MAPK signal transduction pathways in H_2O_2-induced RAECs. Expression levels of (A) p-ERK, (B) p-JNK, (C) p-p38 MAPK and (D) p-Akt proteins in RAECs treated with TFs and Car were quantified using western blotting. Total protein was used as a loading control. n=3. $^{\#\#}$P<0.01 vs. Con group; *P<0.05, **P<0.01 vs. H_2O_2 model group. TFs, total flavonoids; Car, cardamonin; RAECs, rat aortic endothelial cells; p-, phosphorylated; Con, control; Mod, model; Que, quercetin.

pretreated with Car. The expression levels of caspase-3 and Bax were significantly downregulated, and the expression of Bcl-2 was significantly upregulated. In addition, TFs and Car pretreatments attenuated the increase in the Bax/Bcl-2 ratio (Fig. 7G).

TFs and CAR regulate the expression levels of MAPKs and Akt phosphorylation. The Akt and MAPK pathways are important cell signaling pathways. To further demonstrate the antiapoptotic effects of TFs and Car, the roles of the Akt and MAPK pathways were investigated. The results indicated that the expression levels of p-ERK (Fig. 8A), p-JNK (Fig. 8B) and p-p38 MAPK (Fig. 8C) activation were significantly increased in the model group compared with the control group (P<0.01). Pretreatment with TFs and Car significantly attenuated the activation of all three MAPKs compared with the model group (all P<0.05). By contrast, H_2O_2 greatly decreased the phosphorylation of Akt compared with the control group, while treatment with TFs and Car significantly stimulated phosphorylation compared with the model group (P<0.01; Fig. 8D).

Discussion

The present study established an oxidative stress damage model by treating RAECs with H_2O_2 *in vitro* and investigated the protective effects of flavonoids against oxidative stress. The results indicated that TFs and Car could significantly inhibit injury in H_2O_2-induced RAECs, alleviate changes in nuclear morphology and cause cell-protective effects. Endothelial cells are important in maintaining the normal functions of blood vessels by producing and secreting multiple compounds (22). Abnormal endothelial structure and cellular malfunction are the main causes of numerous types of diseases, such as vasculitis, atherosclerosis and thrombosis (23).

ROS play an important role in the pathogenesis of endothelial dysfunction and cardiovascular diseases (24).

The imbalance between the production of ROS and antioxidant defense can result in oxidative stress, which may give rise to metabolic impairment and cell death (25). The present study indicated that TFs and Car could partially suppress oxidative stress by decreasing the generation of ROS and demonstrated their potential to protect RAECs against damage by H_2O_2.

The degree of oxidative damage could be determined by the production of markers of oxidative damage products, such as MDA and LDH. MDA is one of the indexes used to measure the degree of oxidative stress, lipid peroxidation and cell viability. It indirectly reflects the degree of damage due to oxygen free radicals (26). LDH exists in cells and participates in glycolysis, and the activity of LDH can be used as an indicator of the degree of cell membrane damage, which is closely associated with apoptosis. In the present study, the results indicated that H_2O_2 dramatically increased MDA levels and LDH release in RAECs, while these effects were alleviated by treatment with TFs and Car. Therefore, these results suggested that TFs and Car could protect RAECs from oxidative damage.

Mammalian cells have developed an antioxidant defense system to protect against oxidative stress, and the defense system includes some essential antioxidant enzymes, such as SOD and GSH-Px (27,28). SOD activity indirectly reflects the ability to scavenge oxygen free radicals, which plays an important role in regulating the balance between oxidation and antioxidation (3). It can reduce the oxidative damage induced by superoxide anions. GSH-Px has the ability to reduce the toxic by-products of the synthetic pathway by catalyzing peroxidative intermediates to the intermediates used in metabolism (29). The main biological function of GSH-Px is to remove lipid peroxides and H_2O_2 (30). Therefore, the present study analyzed the activities of SOD and GSH-Px. The results demonstrated that TFs and Car enhanced the antioxidant defense system by increasing the activity of SOD and GSH-Px,which is consistent with the results of another study (31).

Oxidative damage induced by excessive ROS generation is known to be a potential inducer of apoptosis. Apoptosis is associated with two family members (Bcl-2 and Bax) and caspase family members (caspase-3, caspase-8 and caspase-9) (32). Bcl-2 family proteins, which usually regulate the mitochondrial pathway of apoptosis, can be divided into two groups: Anti- and pro-apoptotic proteins. Bcl-2 and Bax proteins are the two main members of the Bcl-2 multigene family. Bcl-2 inhibits apoptosis, whereas Bax exerts a proapoptotic effect (33). In the present study, pretreatment with TFs and Car decreased Bax and caspase-3 protein expression and increased Bcl-2 protein expression. The imbalance of the Bax/Bcl-2 ratio switched on the apoptosis process (34). The increased Bax/Bcl-2 ratio transmitted apoptotic signals to caspase-9. Following activation, caspase-9 activates caspase-3, which is a key executor of apoptosis (35). The aforementioned process is known as the mitochondrial apoptotic pathway (36). As expected, the Bax/Bcl-2 ratio was significantly increased in the TF and Car groups compared with the model group of the present study. These results revealed that TFs and Car could regulate the expression of apoptosis-related proteins and inhibit the initiation of apoptosis.

A number of studies have demonstrated that the mechanisms of endothelial cell damage and apoptosis induced by H_2O_2 are associated with the MAPK pathway (36,37). When MAPKs are activated, they can phosphorylate their specific cascade proteins, thus controlling numerous cell activities, including cell proliferation, differentiation and cell death (30,34). The MAPK family, which comprises serine/threonine protein kinases, is involved in the ERK, JNK and p38-MAPK signaling pathways (38). Moreover, p38 and JNK can initiate the mitochondria-dependent intrinsic cell death pathway via the direct phosphorylation of the Bcl-2 family apoptotic protein Bax (39). The present study demonstrated that the phosphorylation levels of JNK, ERK and p38 MAPK were all markedly increased in the model group, while pretreatment with TFs and Car significantly attenuated this elevation. These results suggested that TFs and Car inhibited the activation of the JNK, ERK and p38 MAPK pathways.

Akt, a serine/threonine-protein kinase, plays a key role in multiple cellular processes, such as apoptosis, cell proliferation and migration (40). However, further experiments are needed to verify the results, and the mechanism can provide direction for preventing radiotherapy damage via the ROS pathway.

In conclusion, TFs and Car from LCC had a strong protective effect against H_2O_2-induced oxidative damage and apoptosis of RAECs *in vitro*. Anti-apoptotic activity may mediate mitochondrial Bcl-2 and Bax and inhibit activation of the survival signal-related factor caspase-3. The TFs extracted from LCC could be developed as effective and potential candidate drugs to prevent oxidative stress in the future, and they could also provide a novel direction for preventing antioxidant activity through the ROS pathway caused by radiation damage.

Acknowledgements

Not applicable.

Funding

This work was supported by Zhejiang Chinese Medical Science and Technology Program (grant no. 2019ZB120).

Availability of data and materials

The datasets used and/or analyzed during the current study are available from the corresponding author on reasonable request.

Authors' contributions

JJF conceived the study. FMZ and JJH performed the experiments, analyzed the data, and wrote the manuscript. XJH and JW contributed to the methodology and data analysis. BQZ, SH and ZSD analyzed the data, and wrote and revised the manuscript. JJF acquired funding, contributed to resources, and supervised the study. FMZ and ZSD confirm the authenticity of all the raw data. All authors have read and approved the final manuscript.

Ethics approval and consent to participate

Not applicable.

Patient consent for publication

Not applicable.

Competing interests

The authors declare that they have no competing interests.

References

1. Eelen G, de Zeeuw P, Simons M and Carmeliet P: Endothelial cell metabolism in normal and diseased vasculature. Circ Res 116: 1231-1244, 2015.
2. Figarola JL, Singhal J, Rahbar S, Awasthi S and Singhal SS: LR-90 prevents methylglyoxal-induced oxidative stress and apoptosis in human endothelial cells. Apoptosis 19: 776-788, 2014.
3. Li H, Horke S and Förstermann U: Oxidative stress in vascular disease and its pharmacological prevention. Trends Pharmacol Sci 34: 313-319, 2013.
4. Toghueo K, Marie R and Boyom FF: Endophytes from ethno-pharmacological plants: Sources of novel antioxidants - A systematic review. Biocatal Agric Biotechnol: Nov 14, 2019 (Epub ahead of print).
5. Mahdi A, Kövamees O and Pernow J: Improvement in endothelial function in cardiovascular disease - Is arginase the target? Int J Cardiol 301: 207-214, 2020.
6. Harvey AL, Edrada-Ebel R and Quinn RJ: The re-emergence of natural products for drug discovery in the genomics era. Nat Rev Drug Discov 14: 111-129, 2015.
7. Rao T, Tan Z, Peng J, Guo Y, Chen Y, Zhou H and Ouyang D: The pharmacogenetics of natural products: A pharmacokinetic and pharmacodynamic perspective. Pharmacol Res 146: 104283, 2019.
8. Beretta G and Facino RM: Recent advances in the assessment of the antioxidant capacity of pharmaceutical drugs: From in vitro to in vivo evidence. Anal Bioanal Chem 398: 67-75, 2010.
9. Olszowy M: What is responsible for antioxidant properties of polyphenolic compounds from plants? Plant Physiol Biochem 144: 135-143, 2019.
10. Brainina K, Tarasov A, Khamzina E, Stozhko N and Vidrevich M: Contact hybrid potentiometric method for on-site and in situ estimation of the antioxidant activity of fruits and vegetables. Food Chem 309: 125703, 2020.
11. Wen L, Jiang Y, Yang J, Zhao Y, Tian M and Yang B: Structure, bioactivity, and synthesis of methylated flavonoids. Ann N Y Acad Sci 1398: 120-129, 2017.
12. Chen GL, Fan MX, Wu JL, Li N and Guo MQ: Antioxidant and anti-inflammatory properties of flavonoids from lotus plumule. Food Chem 277: 706-712, 2019.
13. Wei L, Yang M, Huang L and Lin Li J: Antibacterial and antioxidant flavonoid derivatives from the fruits of *Metaplexis japonica*. Food Chem 289: 308-312, 2019.
14. Feng S, Wang L, Belwal T, Li L and Luo Z: Phytosterols extraction from hickory (*Carya cathayensis* Sarg.) husk with a green direct citric acid hydrolysis extraction method. Food Chem 315: 126217, 2020.
15. Xiang L, Wang Y, Yi X, Wang X and He X: Chemical constituent and antioxidant activity of the husk of Chinese Hickory. J Funct Foods 23: 378-388, 2016.
16. Zhu X, Li W, Yu Y, Jiang F and Ding Z: Total flavonoids preparation of the *Carya cathayensis* Sarg. leaves. Zhonghua Zhongyiyao Xuekan 31: 147-149, 2013.
17. Shen Y, Liu NN, Min XU, Zhang K, Jiang FS, Chen JZ, Tian SS and Ding ZS: HPLC determination of the content of the five flavonoid aglycones from the leaves of *Carya cathayensis* Sarg. Yaowu Fenxi Zazhi 33: 804-807, 2013.
18. Cao XD, Ding ZS, Jiang FS, Ding XH, Chen JZ, Chen SH and Lv GY: Antitumor constituents from the leaves of *Carya cathayensis*. Nat Prod Res 26: 2089-2094, 2012.
19. Tian SS, Jiang FS, Zhang K, Zhu XX, Jin B, Lu JJ and Ding ZS: Flavonoids from the leaves of *Carya cathayensis* Sarg. inhibit vascular endothelial growth factor-induced angiogenesis. Fitoterapia 92: 34-40, 2014.
20. Abu Bakar MF, Mohamed M, Rahmat A, Burr SA and Fry JR: Cellular assessment of the extract of bambangan (*Mangifera pajang*) as a potential cytoprotective agent for the human hepatocellular HepG2 cell line. Food Chem 136: 18-25, 2013.
21. Livak KJ and Schmittgen TDL: Analysis of relative gene expression data using real-time quantitative PCR and the 2(-Delta Delta C(T)) method. Methods 25: 402-408, 2001.
22. Chen S, Tang Y, Qian Y, Chen R, Zhang L, Wo L and Chai H: Allicin prevents H_2O_2-induced apoptosis of Huvecs by inhibiting an oxidative stress pathway. BMC Complement Altern Med 14: 321, 2014.
23. Jansen F, Li Q, Pfeifer A and Werner N: Endothelial- and immune cell-derived extracellular vesicles in the regulation of cardiovascular health and disease. JACC Basic Transl Sci 2: 790-807, 2017.
24. Sugamura K and Keaney JF Jr: Reactive oxygen species in cardiovascular disease. Free Radic Biol Med 51: 978-992, 2011.
25. Srivastava KK and Kumar R: Stress, oxidative injury and disease. Indian J Clin Biochem 30: 3-10, 2015.
26. Ma X, Zhang K, Li H, Han S, Ma Z and Tu P: Extracts from *Astragalus membranaceus* limit myocardial cell death and improve cardiac function in a rat model of myocardial ischemia. J Ethnopharmacol 149: 720-728, 2013.
27. Ghaffari H, Ghassam BJ and Prakash HS: Hepatoprotective and cytoprotective properties of Hyptis suaveolens against oxidative stress-induced damage by CCl(4) and H(2)O(2). Asian Pac J Trop Med 5: 868-874, 2012.
28. Kwok HH, Ng WY, Yang MS, Mak NK, Wong RN and Yue PY: The ginsenoside protopanaxatriol protects endothelial cells from hydrogen peroxide-induced cell injury and cell death by modulating intracellular redox status. Free Radic Biol Med 48: 437-445, 2010.
29. Cohen G and Hochstein P: Glutathione peroxidase: The primary agent for the elimination of hydrogen peroxide in erythrocytes. Biochemistry 2: 1420-1428, 1963.
30. Wu P, Ma G, Li N, Deng Q, Yin Y and Huang R: Investigation of in vitro and in vivo antioxidant activities of flavonoids rich extract from the berries of Rhodomyrtus tomentosa(Ait.) Hassk. Food Chem 173: 194-202, 2015.
31. Wu Y, Wang Y and Nabi X: Protective effect of *Ziziphora clinopodioides* flavonoids against H_2O_2-induced oxidative stress in HUVEC cells. Biomed Pharmacother 117: 109156, 2019.
32. Xu F, Ren L, Song M, Shao B, Han Y, Cao Z and Li Y: Fas- and mitochondria-mediated signaling pathway involved in osteoblast apoptosis induced by AlCl3. Biol Trace Elem Res 184: 173-185, 2018.
33. Miura M, Chen XD, Allen MR, Bi Y, Gronthos S, Seo BM, Lakhani S, Flavell RA, Feng XH, Robey PG, *et al*: A crucial role of caspase-3 in osteogenic differentiation of bone marrow stromal stem cells. J Clin Invest 114: 1704-1713, 2004.
34. Lindqvist LM, Heinlein M, Huang DC and Vaux DL: Prosurvival Bcl-2 family members affect autophagy only indirectly, by inhibiting Bax and Bak. Proc Natl Acad Sci USA 111: 8512-8517, 2014.
35. Chen J, Gu Y, Shao Z, Luo J and Tan Z: Propofol protects against hydrogen peroxide-induced oxidative stress and cell dysfunction in human umbilical vein endothelial cells. Mol Cell Biochem 339: 43-54, 2010.
36. Alamdary SZ, Khodagholi F, Shaerzadeh F, Ansari N, Sonboli A and Tusi SK: *S. choloroleuca*, *S. mirzayanii* and *S. santolinifolia* protect PC12 cells from H(2)O(2)-induced apoptosis by blocking the intrinsic pathway. Cytotechnology 64: 403-419, 2012.
37. Wang B, Luo T, Chen D and Ansley DM: Propofol reduces apoptosis and up-regulates endothelial nitric oxide synthase protein expression in hydrogen peroxide-stimulated human umbilical vein endothelial cells. Anesth Analg 105: 1027-1033, 2007.
38. Al-Azayzih A, Gao F, Goc A and Somanath PR: TGFβ1 induces apoptosis in invasive prostate cancer and bladder cancer cells via Akt-independent, p38 MAPK and JNK/SAPK-mediated activation of caspases. Biochem Biophys Res Commun 427: 165-170, 2012.
39. Shi L, Yu X, Yang H and Wu X: Advanced glycation end products induce human corneal epithelial cells apoptosis through generation of reactive oxygen species and activation of JNK and p38 MAPK pathways. PLoS One 8: e66781, 2013.
40. Abbas A, Abdelsamea MM and Gaber MM: Classification of Covid-19 in chest X-Ray images using detrac deep convolutional neural network. Appl Intell 51: 854-864, 2020.